Available online at www.sciencedirect.com
SCIENCE DIRECT®
Journal of Chromatography A, 1009 (2003) 45–59
JOURNAL OF CHROMATOGRAPHY A
www.elsevier.com/locate/chroma

Temperature profiling of polypeptides in reversed-phase liquid chromatography
II. Monitoring of folding and stability of two-stranded α-helical coiled-coils

Colin T. Mant, Brian Tripet, Robert S. Hodges*
Department of Biochemistry and Molecular Genetics, University of Colorado Health Sciences Center, Denver, CO 80262, USA

Abstract

The present study extends the utility of reversed-phase high-performance liquid chromatography (RP-HPLC) to monitor folding and stability of de novo designed synthetic two-stranded α-helical coiled-coils. Thus, we have compared the effect of temperature on the RP-HPLC retention behaviour of both oxidized (two identical five-heptad α-helical peptides linked by a disulfide bridge) and reduced coiled-coil analogues with various amino acids substituted into the hydrophobic core of the coiled-coil. We were able to correlate the RP-HPLC retention behaviour of the oxidized analogues over the temperature range of 10 to 80 °C with the stability of the analogues as determined by conventional thermal and chemical denaturation approaches. In addition, the contribution of a disulfide bridge to coiled-coil stability was highlighted by comparing the elution behaviour of the oxidized and reduced analogues. Overall, we demonstrate the excellent potential of ''temperature profiling'' by RP-HPLC to monitor differences in oligomerization state and protein stability.

Keywords: Temperature effects; Coiled-coils; Polypeptides; Peptides

1. Introduction

In recent years, reversed-phase high-performance liquid chromatography (RP-HPLC) has emerged as a particularly useful physicochemical model of biological systems, where studies have generally centred on correlating the retention behaviour of peptides [1–15] or proteins [16–21] during RP-HPLC with their conformational stability. The assumption with such studies is that the hydrophobic interactions between polypeptides and the non-polar stationary phase characteristic of RP-HPLC [22–24] reflects the hydrophobicity and interactions between non-polar residues which are the major driving forces for protein folding and stability. In addition, the effectiveness of RP-HPLC for such studies is enhanced by the wide choice of stationary phase and/or mobile phase conditions available to the researcher, with temperature adding yet another dimension to such applications [24–27].

In a companion paper [28], we demonstrated the utility of RP-HPLC to monitor dimerization and unfolding of single-stranded amphipathic α-helical peptides over a temperature range of 5 to 80 °C. The logical extension to such a study is to extend this ''temperature profiling'' approach to examination of

*Corresponding author. Tel.: +1-303-315-8837; fax: +303-315-1153.
E-mail address: robert.hodges@uchsc.edu (R.S. Hodges).

0021-9673/03/$ – see front matter
doi:10.1016/S0021-9673(03)00919-1

polypeptides exhibiting higher levels of protein structure, i.e., tertiary and quaternary structure. A minimalistic structural motif well suited to such a study is the two-stranded α-helical coiled-coil, where two amphipathic α-helices form a rod-like structure by coiling around each other into a left-handed superhelix (analogous to a two-stranded rope) stabilized by continuous interhelical contacts between the hydrophobic faces of the helices. In the case of the two-stranded coiled-coil, the hydrophobic positions were identified at regular intervals in a 4–3 (or 3–4) hydrophobic repeat [29], where positions ''a'' and ''d'' in the heptad repeat, denoted by $(abcdefg)_n$, represent hydrophobic amino acid residues. The appeal of the two-stranded α-helical coiled-coil motif as a model protein for assessing the value of temperature profiling by RP-HPLC lies in its simplicity. Thus, it contains only one type of secondary structure, the α-helix, and only two α-helices are required to introduce tertiary and quaternary structure. The burial of hydrophobic surfaces between helices of the coiled-coil mimics the burial of interhelical hydrophobic side-chains in globular proteins; thus providing a model protein with folding characteristics similar to native coiled-coils and globular proteins. In addition, α-helical coiled-coils, made up of two or more α-helices, represent a universal dimerization domain known and/or predicted to be used by nature in well over 200 proteins and encompassing a diverse array of functions, underlying the importance of this motif. Selected reviews and recent publications in this area may be found in Refs. [30–44].

In the present study, we have carried out RP-HPLC on synthetic amphipathic α-helical coiled-coil analogues over a temperature range of 10 to 80 °C at pH 7.0. Observation of the retention behaviour of such coiled-coil motifs subsequently allowed us to make a preliminary assessment of the efficacy of temperature profiling by RP-HPLC in gauging the contribution of specific residues and/or the presence of a disulfide bridge to protein stability and folding of coiled-coils.

2. Experimental

2.1. Materials

HPLC-grade water was prepared by an E-pure water purification system from Barnstead. Acetonitrile was obtained from EM Science (Gibbstown, NJ, USA). Sodium perchlorate was obtained from BDH (Poole, UK).

2.2. Column

RP-HPLC runs were carried out on a PLRP-S polystyrene–divinylbenzene (PS–DVB) column (250×4.6 mm I.D, 5 μm particle size, 100 Å pore size) from Polymer Labs. (Church Stretton, UK).

2.3. Instrumentation

RP-HPLC runs were carried out on an Agilent 1100 Series liquid chromatograph (Agilent Technologies, Little Falls, DE, USA).

Peptide synthesis was carried out on an Applied Biosystems peptide synthesizer Model 430A (Foster City, CA, USA).

2.4. Peptide synthesis and purification

Synthesis of the peptides was carried out by standard solid-phase synthesis methodology using *N-tert*.-butyloxycarbonyl (*t*-Boc) chemistry. Crude reduced peptides were purified by RP-HPLC using a Zorbax 300SB-C_8 column (250×9.4 mm I.D., 6.5 μm, 300 Å) from Agilent Technologies on a Beckman liquid chromatograph. Amino acid analyses of purified peptides were carried out on a Beckman Model 6300 amino acid analyzer (Beckman Instruments, Fullerton, CA, USA) and the correct primary ion molecular masses of peptides were confirmed by mass spectrometry on a Fisons VG Quattro electrospray mass spectrometer (Fisons, Pointe-Claire, Canada).

S-Carboxamidomethyl cysteine peptides were prepared by treating a 1 mg/ml solution of the peptide in 3 m*M* dithiothreitol (DTT), 50 m*M* NH_4HCO_3 buffer (pH 7.8), with a 10-fold excess of iodoacetamide followed by addition of DTT sufficient to quench the excess of iodoacetamide [45]. Disulfide-bridged coiled-coils were formed by overnight air oxidation at room temperature of ~10 mg/ml peptide in 100 m*M* NH_4HCO_3 (pH 8.5).

2.5. Calculations

Data derived from HPLC temperature versus retention time profiles for each of the peptides were plotted using Kaleidagraph (Synergy Software, Reading, PA, USA). The data were curve fitted using the parabolic equation $y = a - [(x - b)^2/c]$, where a, b and c are floated and a = maximum retention time in minutes, $b = T_p$ (see text) and c = scaling factor. The data were weighted to minimize X^2 and maximize r, the correlation coefficient.

3. Results

3.1. Peptide design

Fig. 1 shows the amino acid sequence of the synthetic peptides that were used in this study. The sequence shown at the top represents the polypeptide chain, where single amino acid substitutions are made at position 19a (denoted X) of the sequence, i.e., the substitution site is at the hydrophobic ''a'' position of the central heptad of this 5-heptad sequence. It has been firmly established that the hydrophobic core a and d positions are in large part responsible for defining the stability and oligomerization state of coiled-coils [32,34,41–43,46–59]. Thus, substitutions at position 19a of the sequence allow an accurate determination of the role of position ''a'' in determining the stability and oligomerization state of α-helical coiled-coils. Substitutions at hydrophobic position 19a specifically (i.e., in the central heptad) were chosen, since perturbation of the hydrophobic core in this region has been shown to have the greatest effect on coiled-coil stability [51] and, hence, serves to provide a good test to monitor the effectiveness of temperature profiling by RP-HPLC for monitoring α-helical peptide/protein folding and stability.

Fig. 1 also shows a side view of the model sequence as a two-stranded α-helical coiled-coil with the Cys residues oxidized to form an interchain disulfide bond. The Cys–Gly–Gly sequence at the N-terminus not only permitted disulfide bond formation but also provided a flexible linker that allowed unconstrained helical alignment [41–43,60]. The hydrophobic environment around the site of substitution on the side of the coiled-coil shown in Fig. 1 is mainly defined by Leu15d′ and Leu22d′ (shaded) and by Gln residues at positions 16e, 18g′ and 23e (shaded). The Gln residues were chosen to provide moderately polar, but uncharged, side-chains that prevent charge–charge interactions with the substituted side-chain at position 19a. These Gln residues, along with Gln11g′ also preclude the formation of interhelical e–g′ salt bridges around the substitution site. Three Lys residues were placed at the solvent-exposed f positions of each α-helix to increase the solubility of the peptides at pH 7.0 and to discourage

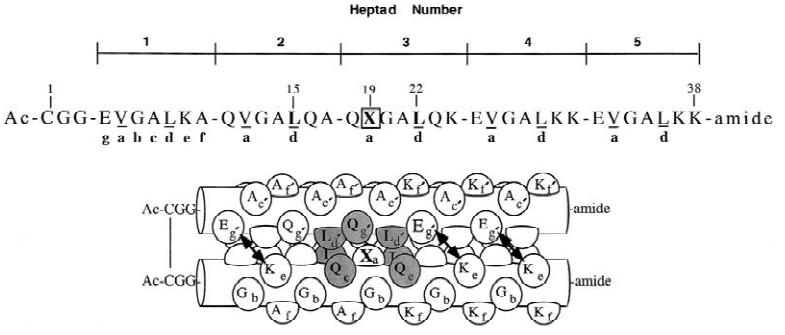

Fig. 1. Model synthetic α-helical coiled-coil protein used in this study. Top: Amino acid sequence of one strand of the model coiled-coil protein. Residues involved in forming the 3–4 hydrophobic repeat at positions a and d are underlined. The substitution site within the sequence is denoted by X and boxed, i.e., residue 19. Ac denotes N^{α}-acetyl and amide denotes C^{α}-amide; the cysteine residue used for disulfide bond formation is located at position 1. The five heptads forming the 35-residue coiled-coil are numbered 1 through 5. The positions of the heptad are labelled ''gabcdef''. Bottom: side-view of the structure of the model α-helical protein in an oxidized (disulfide-bridged), two-stranded oligomerization state. Amino acids defining the microenvironment surrounding the site of amino acid substitution at position 19a (X19a) are shaded. Potential electrostatic interactions occurring across the hydrophobic face are indicated by solid arrows (i to i′+5, g′ to e).

non-specific aggregation. Uncharged Gly and Ala residues were placed at positions b and c to avoid intrahelical ionic interactions with adjacent residues at positions e and g. Interchain electrostatic interactions (i to i′+5 or g′ to e) across the hydrophobic face between Glu in positions 4g′, 25g′ and 32g′ of one helix and Lys in positions 9e, 30e and 37e, respectively, of the adjacent helix (i.e., a total of six such interactions) serve to add stability to the coiled-coil as well as orient the polypeptide chains in an in-register and parallel manner [61,62]. The helical net presentation of the peptide sequence (Fig. 2) highlights the narrow hydrophobic face of the α-helix made up of the core residues at positions a and d of the sequence. This hydrophobic core, as well as determining to a major extent the stability of the coiled-coil, would also represent a preferred binding domain during RP-HPLC [5]. The hydrophobic core consists of four Val and five Leu residues in addition to the residue at position X.

For this initial study, eight peptide analogues were chosen to test the potential of temperature profiling of coiled-coil peptides by RP-HPLC, these analogues being substituted at position 19a by Val, Ala, Thr, Ser, Gly, Glu, Asp and Pro. These eight peptide analogues thus contain single substitutions of amino acids with a range of side-chain characteristics: Val contains a β-branched hydrophobic side-chain; Ala contains a smaller, moderately hydrophobic side-chain; Ser and Thr represent amino acids with polar, uncharged side-chains, the latter also being β-branched; the Gly analogue represents the situation of no side-chain present at the substitution site; Glu and Asp contain acidic side-chains and exhibit a full negative charge at neutral pH; finally, the geometry of the cyclic Pro side-chain makes it extremely disruptive to α-helical secondary structure. The peptide analogues are identified by the three-letter code of the substituted amino acid as well as the presence or absence of a disulfide bridge between individual peptide chains, e.g., Ala_{ox} denotes the two-stranded, disulfide-bridged Ala-substituted analogue, Ala_{red} denotes the Ala analogue in the absence of the disulfide bridge, etc.

3.2. Helicity and stability of peptide analogues

The circular dichroism (CD) spectrum of each oxidized analogue was measured under physiologically relevant, benign buffer conditions and also in 50% trifluoroethanol (TFE) (Table 1). The estimated maximal theoretical molar ellipticity at 222 nm and 25 °C is −34 730 degree cm^2 $dmol^{-1}$ for the 35-residue peptide [42,63,64]. Four of the analogues (Val_{ox}, Ala_{ox}, Thr_{ox}, Glu_{ox}) are 100% α-helical, whilst Ser_{ox}, Gly_{ox}, Asp_{ox} and Pro_{ox} exhibited α-helical values of 94, 79, 18 and 5%, respectively, under benign conditions. These lower values indicate

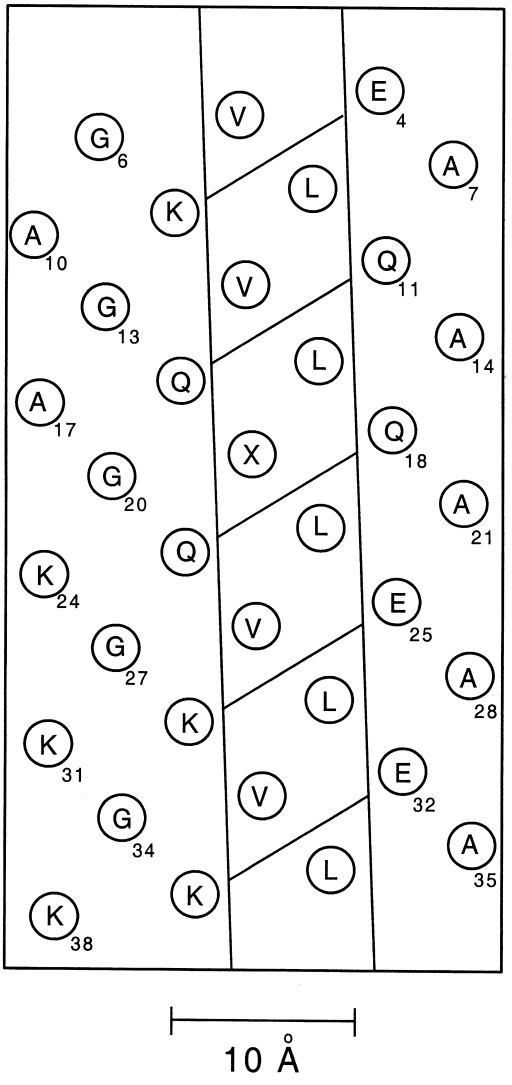

Fig. 2. Helical net representation of model peptide sequence. The hatched area denotes the hydrophobic face of the α-helix, with X denoting the amino acid substitution site.

Table 1
Helicity and stability of disulfide-bridged analogues

Substituted amino acid[a]	$[\theta]_{222}$[b]		$[\theta]_{222/208}$[c]		$[Urea]_{1/2}$[d] (*M*)	T_m[e] (°C)	T_p[g] (°C)	Δt_R[h] (min)
	Benign	50% TFE	Benign	50% TFE				
Val_{ox}	−38 200	−33 100	1.03	0.90	7.56	[122][f]	70	8.0
Ala_{ox}	−34 800	−30 200	1.08	0.85	2.97	62.3	49	4.2
Thr_{ox}	−39 300	−38 900	1.06	0.85	3.18	65.3	53	3.8
Ser_{ox}	−32 800	−29 300	1.03	0.84	1.80	49.3	43	3.1
Gly_{ox}	−27 600	−28 300	1.0	0.82	1.08	38.3	32	2.1
Glu_{ox}	−35 900	−25 300	1.06	0.83	0.60	33.9	36	1.6
Asp_{ox}	−6200	−24 500	0.56	0.80	–	8.4	–	0.1
Pro_{ox}	−1900	−20 300	0.24	0.77	–	–	–	–

[a] Substituted amino acid at position 19a (Fig. 1) denotes the corresponding disulfide-bridged coiled-coil.
[b] Mean residue molar ellipticities at 222 nm (degree cm^2 $dmol^{-1}$); measurements were performed on ~50 μ*M* samples of disulfide-bridged peptide in benign buffer (50 m*M* PO_4, 100 m*M* KCl, pH 7.0) at 25 °C alone or in benign buffer diluted 1:1 (v/v) with trifluoroethanol (TFE), i.e., 50% TFE [42].
[c] A ratio of $[\theta]_{222/208}$ greater than 1.0 is a measure of interacting α-helices and a ratio of ~0.90 represents non-interacting α-helices [47].
[d] $[Urea]_{1/2}$ is the denaturation profile transition midpoint (Fig. 3), i.e., the concentration of urea which causes a 50% loss of peptide α-helicity from that present under benign conditions [42].
[e] T_m is the midpoint of thermal denaturation profiles in benign buffer (50 μ*M* KH_2HPO_4, 100 m*M* KCl, pH 7.0), i.e., the temperature at which 50% of the original α-helicity of the peptide analogue has been lost compared to α-helical content at 5 °C [42].
[f] T_m value for Val_{ox} extrapolated from measured $[urea]_{1/2}$ values of other disulfide-bridged analogues [42].
[g] T_p is the transition point of the change in retention time of an oxidized analogue relative to its retention time at 10 °C (Fig. 4B).
[h] Δt_R is the maximum difference in retention time of an oxidized analogue relative to its retention time at 10 °C (Fig. 4B).

that the peptide populations of these analogues were either not completely in the folded state, or in the case of Asp_{ox} and Pro_{ox}, were essentially in the unfolded state under benign conditions. Under these benign conditions, the ratio of ellipticities (222/208 nm) was greater than 1.0 for Val_{ox}, Ala_{ox}, Thr_{ox}, $Ser_{ox,}$ and Glu_{ox} [i.e., the analogues which exhibited molar ellipticities comparable to the theoretical maximum (Table 1)], which is indicative of the presence of interacting α-helices [47,65]. Interestingly, when ellipticity was measured in the presence of helix-inducing solvent TFE, even the Asp_{ox} and Pro_{ox} analogues now exhibited considerable α-helicity, even compared to the remaining analogues (Table 1). High concentrations of TFE (40–50%) have been viewed as useful mimics of the hydrophobic environment characteristic of RP-HPLC (highly non-polar stationary phase, non-polar organic modifier in the mobile phase) [5] and hence such results strongly suggest that the analogues are bound to the reversed-phase stationary phase in their maximally helical conformation. Indeed, it is well established that, in a similar manner to TFE, the hydrophobic environment of RP-HPLC induces helical conformation in potentially helical peptides [66,67]. Also from Table 1, the ratio of ellipticities of all seven analogues in the presence of 50% TFE now ranges from 0.77 to 0.90, which is characteristic of non-interacting α-helices, i.e., due to the disruptive effect of TFE on tertiary and quaternary structure [47,65,68], even the five analogues (Val_{ox}, Ala_{ox}, Thr_{ox}, Glu_{ox} and Ser_{ox}) which clearly exhibited a coiled-coil conformation under benign conditions had lost this coiled-coil motif in this more hydrophobic environment. Significantly, such results also suggest that none of the disulfide-bridged analogues will maintain coiled-coil structure when bound to the hydrophobic RP-HPLC stationary phase, i.e., in a similar manner to the effect of TFE, all seven analogues will be bound in an extended α-helical conformation to the hydrophobic stationary phase of a reversed-phase column due to the disruptive nature of such phases to polypeptide tertiary and quaternary structure and ability to stabilize secondary α-helical structure.

Urea denaturation curves obtained with Val_{ox}, Ala_{ox}, Thr_{ox}, Ser_{ox}, Gly_{ox} and Glu_{ox} are shown in Fig. 3, with the $[urea]_{1/2}$ values reported in Table 1. The analogues exhibited a range of stabilities, with Val_{ox} (substituted at position 19a by a β-branched hydrophobic side-chain) showing by far the highest

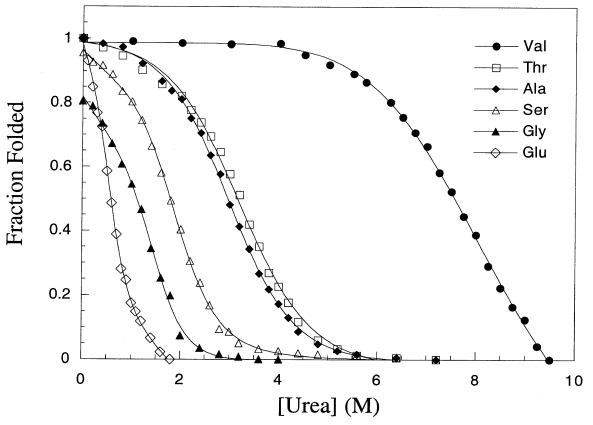

Fig. 3. Urea denaturation profiles of oxidized model α-helical coiled-coil proteins. Denaturations were carried out at 25 °C in 0.1 *M* KCl, 0.05 *M* PO_4 (pH7) buffer containing urea. The fraction folded (f_f) of each peptide was calculated as described in Experimental. Each peptide was analyzed at ~50 μ*M* concentration. The 38-residue, two-stranded, disulfide-bridged peptides are denoted by the residue substituted at position 19a in each polypeptide chain (Fig. 1). Adapted from Ref. [41].

stability ($[urea]_{1/2}$ value of 7.56 *M*), followed by Ala_{ox} (substituted by a small, non-polar side-chain) and Thr_{ox} (substituted by a β-branched uncharged polar side-chain) showing the next highest (and similar) $[urea]_{1/2}$ values (2.97 and 3.18 *M*, respectively) and Glu_{ox} (substituted by a destabilizing negatively charged side-chain) showing a value of just 0.60 *M*. Due to the relatively negligible helical content of Asp_{ox} and Pro_{ox} at room temperature, it was not possible to obtain $[urea]_{1/2}$ values for these analogues, indicating the destabilizing effect of these substitutions on coiled-coil structure.

Table 1 also shows the results of thermal denaturation of the disulfide-bridged analogues, the stabilities of the analogues, as expressed by their T_m values, again showing a similar trend of decreasing stabilities as observed for the $[urea]_{1/2}$ values, with the highest measured T_m values seen for Ala_{ox} and Thr_{ox} (62.3 and 65.3 °C, respectively) to just 33.9 °C for Glu_{ox}. It was also possible to obtain a T_m value for Asp_{ox}, since at the starting temperature of 5 °C for such studies, the Asp_{ox} became highly helical compared to only 18% helicity at 25 °C (Table 1) [42]. In addition, all analogues, with the exception of Pro_{ox}, exhibited 222/208 nm ellipticity ratios >1.0 at 5 °C, indicating the presence of interacting α-helices (i.e., a coiled-coil) at this low starting temperature (data not shown). It should be noted that, due to the high inherent stability of the coiled-coil scaffold, it is not always possible to obtain thermal denaturation profiles for highly stable coiled-coil analogues, e.g., Val_{ox}. However, it has been shown that the T_m value for such an analogue may be extrapolated from measured $[urea]_{1/2}$ values since there is a linear correlation between T_m and $[urea]_{1/2}$ values for the other analogues [42]; hence the extrapolated value of $T_m = 122$ °C for Val_{ox} (Table 1).

From the results shown in Table 1 and Fig. 3, the eight peptide analogues exhibit a useful range of helicities and stabilities for an initial test of our temperature profiling approach to monitor coiled-coil folding and stability.

3.3. Effect of temperature on RP-HPLC retention behaviour of peptide analogues

Fig. 4A shows the effect of increasing temperature on RP-HPLC retention behaviour of oxidized, two-stranded α-helical peptide analogues over the range of 10–80 °C. A random coil peptide standard, RX2 (Ac–Lys–Tyr–Gly–Leu–Gly–Gly–Ala–Gly–Gly–Leu–Lys–amide), was also included to gauge the effects of increasing temperature on RP-HPLC of a polypeptide with negligible secondary structure. At 80 °C, the disulfide-bridged peptides are eluted, as expected, in order of their hydrophobicity at the substitution site, i.e., the order of retention times is Val>Ala>Gly peptide. The retention behaviour of the random coil peptide standard, RX2, is showing an expected linear decrease in retention time with increasing temperature. As the temperature increases, the mobile phase viscosity is lowered and mass transfer is improved significantly. At 80 °C, the large hydrophobicity difference between the α-helical peptides [with the preferred binding domain consisting of four Val, five Leu residues and the position X residue per polypeptide chain (Fig. 2)] and the random coil peptide (with only two Leu, one Tyr and one Ala residue) is as expected (Fig. 4A). Interestingly, the retention behaviour of the helical peptides with a decrease in temperature appears more anomalous. Thus, as the temperature decreases from 80 °C, the peptides become less retentive and their order of

elution at 10 °C is opposite to that at 80 °C. In other words, the most hydrophobic Val peptide is eluted first, followed by the Ala peptide and, finally, the Gly peptide at 10 °C.

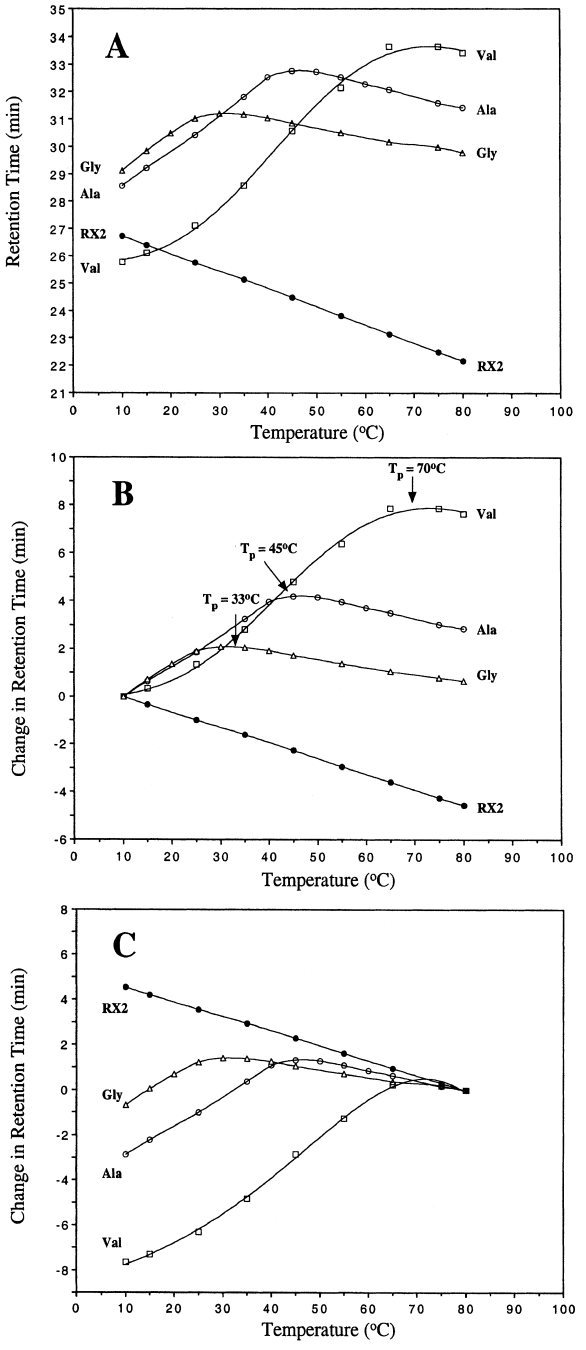

In order to present more clearly the differences in retention behaviour of the peptide analogues over the temperature range, the data have been normalized by subtracting each analogue retention time at a specific temperature from that of its retention time at 10 °C ($\Delta t_R = t_R - t_R 10$ °C; Fig. 4B) or its retention time at 80 °C ($\Delta t_R = t_R - t_R 80$ °C; Fig. 4C). Plotting the retention data in this manner highlights dramatic differences in retention behaviour of the oxidized analogues with increasing or decreasing temperature. Thus, Val_{ox}, Ala_{ox}, and Gly_{ox}, all initially exhibited an increase in retention time with increasing temperature relative to their t_R values at 10 °C (panel B), albeit to differing extents, ranging from a maximum Δt_R value of 8.0 min for Val_{ox} to just 2.1 min for Gly_{ox}. In addition, these oxidized analogues show a range of temperatures at which this maximum Δt_R value (or transition point) occurs. Calculated values for these temperatures at the transition points (T_p; see Experimental for description of calculations) ranged from 70 °C for Val_{ox} to 33 °C for Gly_{ox}. Similarly, the other analogues showed different temperature profiles with different T_p and Δt_R values (Table 1). From Fig. 4C, which shows the effect of normalizing the data to 80 °C, the retention time of the peptides track more closely the retention behaviour of the random coil peptide before showing large deviations. The results of Fig. 4B and C both show that the deviations from that of the random coil peptide are related to the relative order of stability of the two-stranded coiled-coil peptides (Fig. 3) where the

Fig. 4. Effect of temperature on RP-HPLC of disulfide-bridged (oxidized) α-helical peptide analogues. (A) Effect of temperature on retention time of peptides. (B) Effect of temperature on retention behaviour of peptides presented as analogue retention time at a specific temperature minus its retention time at 10 °C ($t_R - t_R 10$ °C); T_p denotes the temperature at the inflexion point of the profiles. (C) Effect of temperature on retention behaviour of peptides presented as analogue retention time at a specific temperature minus its retention time at 80 °C ($t_R - t_R 80$ °C). The sequence of the random coil peptide, RX2, is Ac–Lys–Tyr–Gly–Leu–Gly–Gly–Ala–Gly–Gly–Leu–Lys–amide. Column: see Experimental. Conditions: linear A–B gradient (2% B/min, equivalent to 1% acetonitrile/min) at a flow-rate of 1 ml/min, where eluent A is 50 m*M* aq. NaH_2PO_4, pH 7.0, and eluent B is A in 50% aq. acetonitrile, both eluents containing 100 m*M* $NaClO_4$. Val, Ala and Gly denote the residues substituted at position 19a in each polypeptide chain of the two-stranded, disulfide-bridged, α-helical coiled-coil (Fig. 1).

$[urea]_{1/2}$ values are 7.6, 3.0 and 1.1 *M* for Val_{ox}, Ala_{ox} and Gly_{ox} respectively (Fig. 3, Table 1).

Fig. 5A shows the effect of increasing temperature on the RP-HPLC of the reduced analogues Val_{red} and Ala_{red} compared to the disulfide-bridged peptides Val_{ox} and Ala_{ox}. It is obvious that the retention behaviour of the reduced peptides is dramatically different from the disulfide-bridged peptides. At 80 °C, the retention behaviour is based on relative hydrophobicity, as expected. For example, the Val_{ox} peptide has two polypeptide chains joined by a disulfide bridge compared to Val_{red} which has just one polypeptide chain. Thus, Val_{ox} has twice the hydrophobicity of the reduced peptide and is significantly more retentive. This is not the case at 10 °C where the disulfide-bridged peptides are eluted substantially prior to their reduced analogues. This strongly suggests that the oxidized peptides are folding during chromatography, burying hydrophobic residues to cause this retention behaviour. The retention times of the peptides have been subsequently normalized to 10 °C (Fig. 5B) to show this effect more clearly.

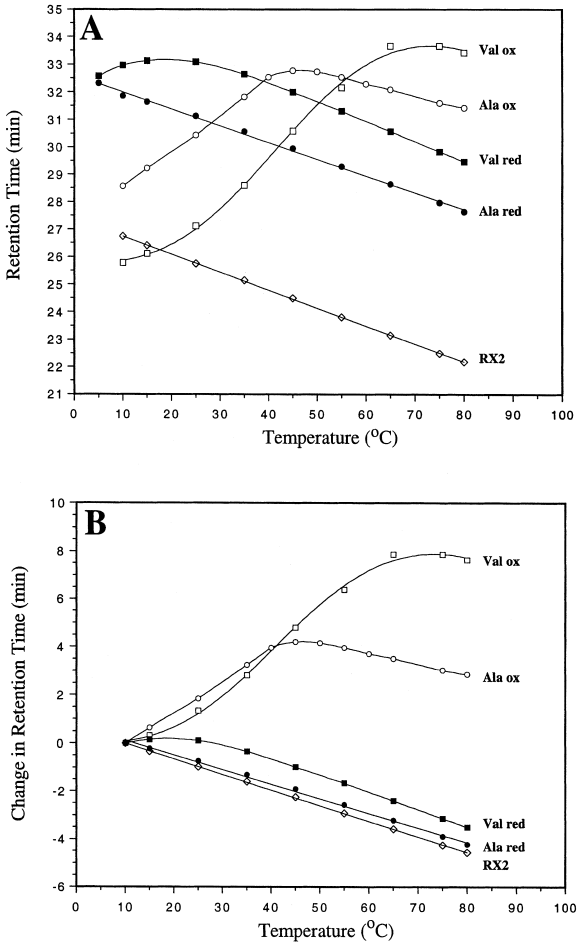

Fig. 5. Comparison of effect of temperature on RP-HPLC of reduced and oxidized α-helical peptide analogues. (A) Effect of temperature on retention times of peptides. (B) Effect of temperature on retention behaviour of peptides at a specific temperature minus its retention time at 10 °C ($t_R - t_R$10 °C). The sequence of random coil peptide standard, RX2, is shown in Fig. 4. Column and conditions: see Fig. 4. Val and Ala denote the residues substituted at position 19a of the polypeptide chain; ox represents the oxidized, two-stranded, α-helical coiled-coil and red represents the absence of a disulfide bridge (Fig. 1).

Unlike the Val-substituted analogue (Val_{red}), the Ala peptide exhibits an immediate and similar decrease in retention time with increasing temperature to that of the random coil peptide standard, RX2. That is, the disulfide bridge clearly has a dramatic effect on the retention behaviour. It is well documented that a disulfide bridge between the two helical strands of a coiled-coil has a dramatic effect on the stability of the coiled-coil [34,69,70].

Fig. 6 presents a visual comparison of the characteristic effect of increasing temperature on RP-HPLC of oxidized versus the reduced state, specifically Ala_{ox} (Fig. 6, left) versus Ala_{red} (Fig. 6, right). Note that, although the profiles illustrated were obtained on a silica-based RP-HPLC column, compared to the polystyrene column from which the remainder of reported data were obtained, results obtained on either type of column were essentially identical. From Fig. 6 (left), the retention time of Ala_{ox} increases on raising the temperature from 10 to 45 °C, before decreasing again at 80 °C (compare to graphical representation in Fig. 4A). In contrast, the retention time of Ala_{red} (Fig. 6, right) consistently decreases with increasing temperature. Thus, as shown graphically in Fig. 5A, the elution times of Ala_{ox} and Ala_{red} are reversed at the lowest (10 °C) and highest (80 °C) temperatures. Interestingly, Ala_{ox} exhibits similar peak width ($w_{1/2} = 0.51$ min) at 10 and 45 °C but the peak narrows significantly at 80 °C ($w_{1/2} = 0.22$ min), concomitant with more than a doubling of peak height. In contrast, the peak width

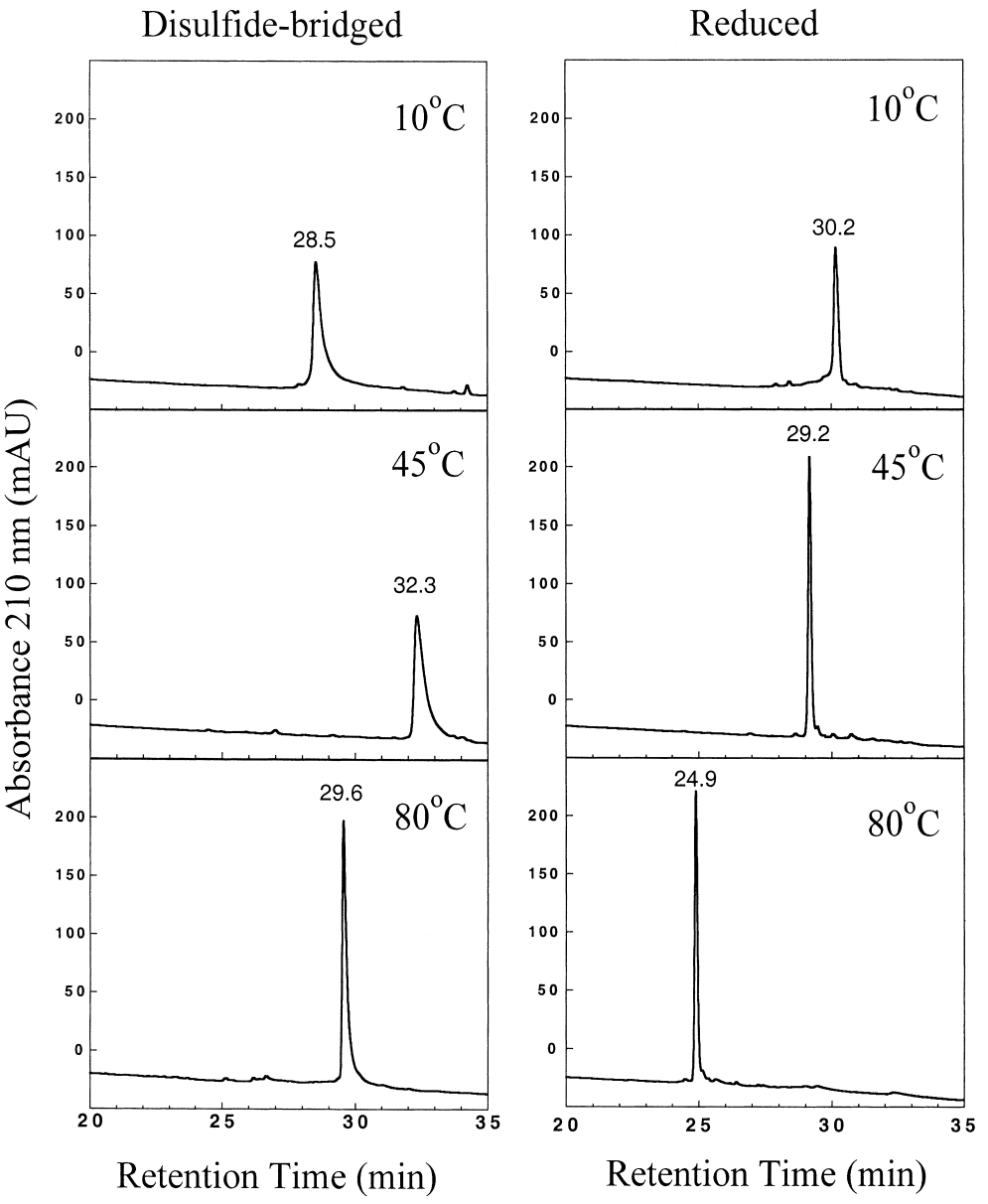

Fig. 6. Effect of temperature on RP-HPLC of Ala_{ox} (disulfide-bridged Ala-peptide analogue) and Ala_{red} (reduced Ala-peptide analogue). Column: Zorbax Eclipse XDB-C_8 (150×4.6 mm I.D., 5 μm particle size, 100 Å pore size) from Agilent Technologies (Little Falls, DE, USA). Conditions: linear A–B gradient (2% B/min, equivalent to 1% acetonitrile/min) at a flow-rate of 1 ml/min, where eluent A is 50 m*M* aq. NaH_2PO_4, pH 7.0, and eluent B is A in 50% aq. acetonitrile, both eluents containing 100 m*M* $NaClO_4$.

of Ala_{red} decreases significantly between 10 °C ($w_{1/2}$ = 0.21 min) and 45 °C ($w_{1/2}$ = 0.13 min), with peak height essentially doubling on raising the temperature from 10 to 45 °C, then peak height and peak width remaining similar in the 45 to 80 °C range.

3.4. Correlation of RP-HPLC temperature profiles of peptides with biophysical parameters

Fig. 7 compares parameters derived from the temperature profiles shown in Fig. 4A and reported in Table 1 (Δt_R and T_p values) with the denaturation data ($[urea]_{1/2}$ and T_m values) of the oxidized, two-stranded peptide analogues. Only the stablest peptide analogues are compared in Fig. 6, i.e., Asp_{ox} and Pro_{ox} are excluded, since these latter analogues either do not form a coiled-coil (Pro_{ox}) or only exhibit marginal stability (Asp_{ox}). From Fig. 7, the transition point values (T_p) obtained from RP-HPLC data (Fig. 4A) show excellent correlations with the thermal denaturation midpoint values (T_m; $r = 0.991$; Fig. 7A) and the urea denaturation midpoint values ($[urea]_{1/2}$; $r = 0.992$; Fig. 7C). Interestingly, the Δt_R values of the analogues also correlate well with the biophysical parameters ($r = 0.994$ for correlations with both T_m values (Fig. 7B) and $[urea]_{1/2}$ values (Fig. 7D). These observations imply that, for these oxidized, two-stranded α-helical model peptides, the maximum retention times attained in RP-HPLC (a measure of apparent peptide hydrophobicity) as well as the temperature at which this maximum retention time occurs are both related to the stability of the coiled-coils in solution as measured through thermal and chemical denaturation (Table 1).

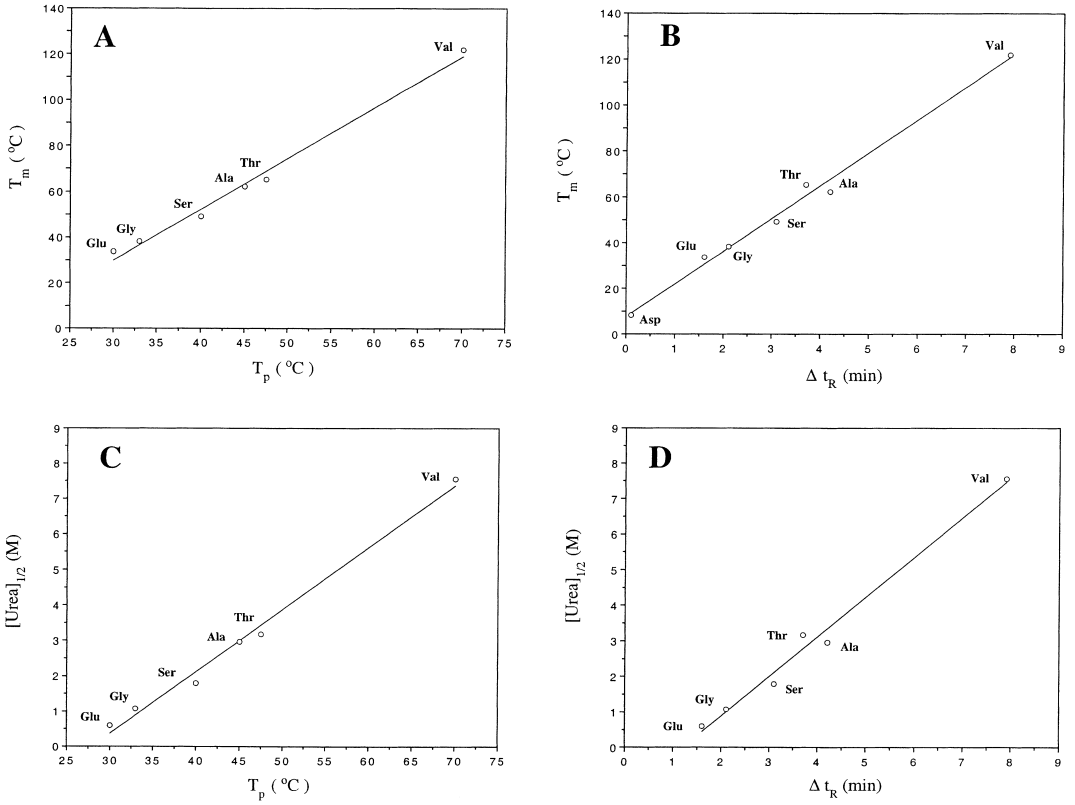

Fig. 7. Correlation of RP-HPLC temperature profiling transition points (T_p) and Δt_R values of oxidized peptide analogues with coiled-coil stability. (A) and (C) Correlation of thermal denaturation midpoint, T_m, and $[urea]_{1/2}$ value with T_p. (B) and (D) Correlation of T_m and $[urea]_{1/2}$ value, with Δt_R values. Urea and thermal denaturation transition midpoint data for the two-stranded, disulfide-bridged analogues are shown in Table 1. The RP-HPLC temperature profiling transition points, T_p, and Δt_R values were calculated from the plots shown in Fig. 4B, as described in Experimental. The amino acids shown by their three-letter codes denote the substituted residues at position *19a* in each polypeptide chain of the two-stranded, disulfide-bridged, α-helical coiled-coil (Fig. 1).

4. Discussion

4.1. Hypothesis for temperature profiling of two-stranded α-helical coiled-coils

Based on the RP-HPLC temperature profiles of the helical peptide analogues shown in Figs. 4 and 6, as well as the helicity and stability data reported in Table 1 and compared in Fig. 7, the following hypothesis for correlating RP-HPLC retention behaviour with peptide conformation and stability is postulated (Fig. 8).

It is known that, although peptides are eluted from a reversed-phase column mainly by an adsorption/desorption mechanism [22,24], even a peptide strongly bound to a reversed-phase matrix will partition between the aqueous mobile phase in equilibrium with its bound state in a narrow range of acetonitrile concentrations during gradient elution. Depending on the stability of a crosslinked coiled-coil, as well as the temperature of its environment, the concentration of the coiled-coil in the mobile phase will vary from: mainly native folded two-stranded coiled-coil; a mixture of coiled-coil and single-stranded α-helix; or single-stranded α-helix only.

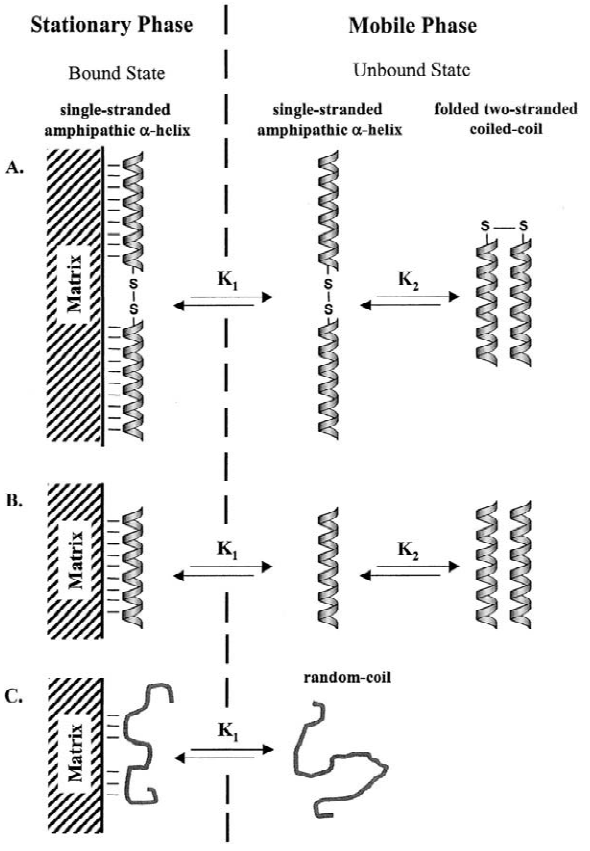

Fig. 8. Proposed mechanism of folding of two-stranded α-helical coiled-coils during temperature profiling in RP-HPLC. See discussion in Section 4.1 for description.

From Fig. 8A, at low temperature, the main component in the mobile phase during partitioning is the folded disulfide-bridged two-stranded α-helical coiled-coil, i.e., the concentration of single-stranded α-helix in solution is low and the concentration of folded coiled-coil is high. However, at higher temperatures the equilibrium favours the unfolded coiled-coil (i.e., the single-stranded α-helix) more and more as the coiled-coil is increasingly unfolded with increasing temperature, thus increasing the concentration of the single-stranded α-helix in solution concomitant with a decrease in coiled-coil concentration. At high temperatures, only the single-stranded α-helix is present in solution due to the complete loss of tertiary/quaternary structure of the coiled-coil. Finally, whether in the single-stranded α-helical state or the folded coiled-coil state in the mobile phase, the bound state is always in the single-stranded α-helical state since the hydrophobicity of the stationary phase disrupts tertiary/quaternary structure but stabilizes secondary structure in the case of amphipathic α-helices. Note that the coiled-coil state must be fully disrupted for rebinding of the non-polar face of the α-helix to the hydrophobic stationary phase. Thus, rebinding is faster at higher temperatures where the single-stranded α-helix is the only species in the mobile phase. During partitioning, the single-stranded α-helix is released from the matrix into solution and, depending on the temperature, refolds to the two-stranded coiled-coil native state.

Fig. 8B now illustrates the putative behaviour of the α-helical peptide analogues in the absence of the stabilizing disulfide bridge between the individual strands, i.e., the reduced analogues. Thus, again depending on the temperature of the environment and the stability of the two-stranded coiled-coil, the

conformation in the mobile phase is one of two possibilities: mainly monomeric α-helix or a mixture of monomeric α-helix and dimeric two-stranded α-helical coiled-coil. Fig. 8C shows the interaction of the random coil peptide where there is no conformational change in the mobile phase. That is, the random coil exists in solution and has no structure when bound. Thus, there is a linear relationship of retention behaviour with increasing temperature for random-coil peptides. Due to the effects of temperature on solvent viscosity and mass transfer the net effect is decreasing retention time with increasing temperature (Fig. 4).

Fig. 9 shows the change in retention time when the disulfide-bridged and reduced peptides are normalized to 80 °C and these data are subtracted from the retention behaviour of the random coil peptides. In other words, we are observing the change in retention behaviour of the various coiled-coil peptides relative to the random coil peptide. This plot in essence gives the increasing concentration of the two-stranded α-helical coiled-coil as a function of temperature. Clearly the more stable the coiled-coil the more coiled-coil structure is observed at lower temperatures. In the reduced peptides, coiled-coil is only observed at temperatures below 25 °C.

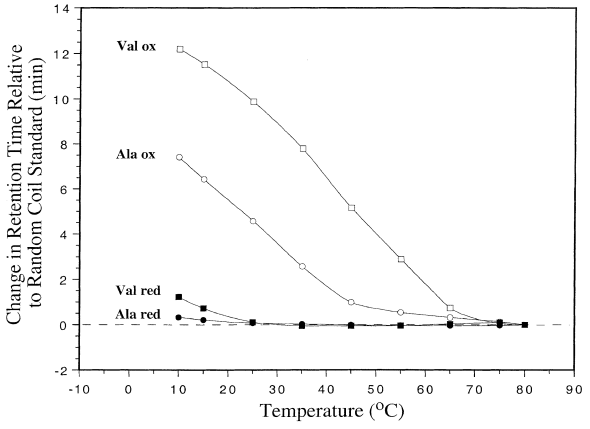

Fig. 9. Effect of temperature on RP-HPLC retention behaviour of reduced and oxidized α-helical peptides: normalization to retention time of random coil peptide standard RX2. The profiles were produced through the expression (t_RRX2 − t_RRX2 at 80 °C) minus (t_R − t_R80 °C) of a specific peptide. The sequence of RX2 is shown in Fig. 4. Column and conditions: see Fig. 4. Val and Ala denote the residues substituted at position 19a of the polypeptide chain; ox represents the oxidized, two-stranded, α-helical coiled-coil and red represents the absence of a disulfide bridge (Fig. 1).

4.2. Monitoring of folding and stability of two-stranded α-helical coiled-coils by temperature profiling in RP-HPLC

Taking Val_{ox} as an example in Fig. 4B, the initial increase in retention time with temperature may be explained by a gradual disruption of its coiled-coil (i.e., the equilibrium between coiled-coil and extended α-helix in solution increasingly favours the latter), concomitant with more exposure of hydrophobic residues. At a certain temperature or transition temperature (T_p = 70 °C for Val_{ox}), the dominating species of Val_{ox} is the fully extended form in solution; that is, there is an increased exposure of hydrophobic residues and hence a maximum retention time (expressed here as the maximum retention time attained compared to 10 °C; Δt_R) is reached when this increased exposure of hydrophobic residues is counterbalanced by the increasing general temperature effects on peptide retention behaviour. From Fig. 6, the effect of temperature on peak shape of Ala_{ox} may also be rationalized in terms of the equilibrium between coiled-coil and extended α-helix in solution at different temperatures. Thus, between 10 and 45 °C, a large concentration of the coiled-coil species is present in solution, perhaps dominating over much of this temperature range the coiled-coil–extended α-helix equilibrium and, hence, resulting in relatively broad peak widths. Above 45 °C (the T_p value for Ala_{ox}), there is a steady shift favouring the extended α-helix species until, at 80 °C, only the latter species is present in solution and the peak behaviour is consistent with the general effects of temperature, i.e., reduced retention time, decreased peak width and increased peak height due substantially to the increase in mass transfer between stationary and mobile phases as the temperature is increased.

Apart from affecting RP-HPLC retention time, the hydrophobicity of the non-polar face of the individual amphipathic α-helical strands of the oxidized analogues also affects coiled-coil stability [41–43]. Thus, as a general rule, the more hydrophobic the substituted residue in the non-polar face of the peptide, the more stable the coiled-coil [41–43] and,

hence, the higher the temperature required to destabilize it as expressed both by the range of T_m (and, indeed, $[urea]_{1/2}$) values of the oxidized analogues as well as the RP-HPLC-derived T_p values (Table 1). Concomitant with these parameters, a decrease in hydrophobicity of the substituted residue in the non-polar face of the amphipathic peptides leads to a decrease in RP-HPLC retention times relative to those observed at 10 °C (Δt_R) as the non-polar face is increasingly exposed with a rise in temperature. Considering the marginal stability of Asp_{ox} ($T_m = 8.4$ °C and a $[urea]_{1/2}$ value could not be obtained; Table 1), the helix–helix interaction detected during RP-HPLC is a testament to the sensitivity of the temperature profiling approach to assessing α-helical coiled-coil stability. This sensitivity is likely aided by the high concentration of the peptides which is obtained during loading of the reversed-phase column in the absence of organic modifier even though the amount of sample loaded is small.

Concerning the profiles of the reduced analogues (Val_{red} and Ala_{red} only are shown in Fig. 5), there is no dimerization detected during chromatography of the majority of amphipathic α-helices in the absence of the disulfide bridge, supporting earlier non-RP-HPLC-based work in our laboratory clarifying the importance of this bridge to the stability of these very small two-stranded α-helical coiled-coils with the substituted site in the centre of the coiled-coil interface [70]. Interestingly, some dimerization of the most stable α-helix, Val_{red}, was apparent in Fig. 4B and confirmed in Fig. 9, albeit to a much lesser degree than the crosslinked analogue. Thus, the T_p values for Val_{ox} and Val_{red} were 70 and 20 °C, respectively. Interestingly, although not apparent in the profiles shown in Fig. 5, even the Ala_{red} peptide was detected to exhibit some dimerization at low temperature in the normalized data of Fig. 9. Such results again indicate the sensitivity of this RP-HPLC-based profiling approach to assessing helix–helix interaction as well as underlining the contribution of the disulfide bridge to coiled-coil stability.

The results in Fig. 9, where the retention data have been normalized to 80 °C and subtracted from the retention behaviour of the random coil peptide, clearly show that temperature profiling monitors the change in conformational state. That is, for the reduced peptides Val_{red} and Ala_{red}, the peptides exist as monomeric α-helices and there is no change in conformation in the temperature range 25–80 °C. Thus, the rate of change in retention behaviour with temperature is identical to that of the random coil peptide. An α-helical conformation that is stable over the temperature range 10–80 °C will parallel the behaviour of a random coil peptide. It should be noted that such a conclusion is also supported by the elution profiles of Ala_{red} shown in Fig. 6 (right). Thus, with the monomer–dimer equilibrium heavily favouring the monomeric species even at 10 °C and being the only species present at higher temperatures, the effect on Ala_{red} peak elution behaviour of raising the temperature is as would be expected for a random coil peptide, i.e., a decrease in peptide retention time and peak width and a concomitant increase in peak height with increasing temperature.

5. Conclusions

In the present study, we have extended our initial assessment of the value of temperature profiling in RP-HPLC of peptide conformation and unfolding [28] to that of monitoring the folding and stability of two-stranded α-helical coiled-coils. Observation of the effect of temperature (10 to 80 °C) on the elution behaviour of oxidized (disulfide-bridged) and reduced coiled-coil analogues clearly illustrated the excellent potential of this temperature profiling approach to monitor differences in oliogomerization state and protein stability as well as highlighting the contribution of a disulfide bridge to stabilizing the folded state.

Acknowledgements

This work was supported by an NIH grant to R.S.H. (GM 61855).

References

[1] M.L. Heinitz, E. Flanigan, R.C. Orlowski, F.E. Regnier, J. Chromatogr. 443 (1988) 229.

[2] K.D. Lork, K.K. Unger, H. Bruckner, M.T.W. Hearn, J. Chromatogr. 476 (1989) 135.
[3] A.W. Purcell, M.I. Aguilar, M.T.W. Hearn, J. Chromatogr. 476 (1989) 125.
[4] D.E. Henderson, J.A. Mello, J. Chromatogr. 449 (1990) 79.
[5] N.E. Zhou, C.T. Mant, R.S. Hodges, Peptide Res. 3 (1990) 8.
[6] V. Steiner, M. Schär, K.O. Börnsen, M. Mutter, J. Chromatogr. 586 (1991) 43.
[7] M.I. Aguilar, S. Mougos, J. Boublik, J. Rivier, M.T.W. Hearn, J. Chromatogr. 646 (1993) 53.
[8] A.W. Purcell, M.I. Aguilar, M.T.W. Hearn, J. Chromatogr. A 711 (1995) 61.
[9] A.W. Purcell, M.I. Aguilar, M.T.W. Hearn, J. Chromatogr. A 711 (1995) 71.
[10] A.W. Purcell, M.I. Aguilar, R.E.H. Wettenhall, M.T.W. Hearn, Peptide Res. 8 (1995) 160.
[11] S.E. Blondelle, B. Forood, E. Pérez-Payá, R.A. Houghten, Int. J. Biochromatogr. 2 (1996) 133.
[12] E. Lazoura, I. Maidonis, E. Bayer, M.T.W. Hearn, Biophys. J. 72 (1997) 238.
[13] T.H. Lee, P.E. Thompson, J. Peptide Res. 49 (1997) 394.
[14] D.L. Steer, P.E. Thompson, S.E. Blondelle, R.A. Houghten, M.I. Aguilar, J. Peptide Res. 51 (1998) 401.
[15] T. Wieprecht, S. Rothemund, M. Bienert, E. Krause, J. Chromatogr. A 912 (2001) 1.
[16] C.T. Mant, N.E. Zhou, R.S. Hodges, J. Chromatogr. 476 (1989) 363.
[17] K. Benedeck, J. Chromatogr. 646 (1993) 91.
[18] R. Rosenfeld, K. Benedek, J. Chromatogr. 632 (1993) 29.
[19] R.S. Hodges, B.-Y. Zhu, N.E. Zhou, C.T. Mant, J. Chromatogr. A 676 (1994) 3.
[20] K.L. Richards, M.I. Aguilar, M.T.W. Hearn, J. Chromatogr. A 676 (1994) 17.
[21] Y.B. Yu, K.C. Wagschal, C.T. Mant, R.S. Hodges, J. Chromatogr. A 890 (2000) 81.
[22] C.T. Mant, R.S. Hodges (Eds.), High-Performance Liquid Chromatography of Peptides and Proteins: Separation, Analysis and Conformation, CRC Press, Boca Raton, FL, 1991.
[23] C.T. Mant, R.S. Hodges, Methods Enzymol. 271 (1996) 3.
[24] C.T. Mant, R.S. Hodges, in: K.M. Gooding, F.E. Regnier (Eds.), HPLC of Biological Macromolecules, Marcel Dekker, New York, 2002, p. 433.
[25] J.J. Kirkland, J.W. Henderson, J.J. DeStefano, M.A. van Straten, H.A. Claessens, J. Chromatogr. A 762 (1997) 97.
[26] C.T. Mant, L.H. Kondejewski, P.J. Cachia, O.D. Monera, R.S. Hodges, Methods Enzymol. 289 (1997) 426.
[27] C. McNeff, L. Zigan, K. Johnson, P.W. Carr, A. Wang, A.M. Weber-Main, LC·GC 18 (2000) 514.
[28] C.T. Mant, Y. Chen, R.S. Hodges, J. Chromatogr. A (2003) in press.
[29] J. Sodek, R.S. Hodges, L.B. Smillie, L. Jurasek, Proc. Natl. Acad. Sci. 69 (1972) 3800.
[30] C. Cohen, D.A. Parry, Proteins 7 (1990) 1.
[31] T. Alber, Curr. Opin. Genet. Dev. 2 (1992) 205.
[32] R.S. Hodges, Curr. Biol. 2 (1992) 122.
[33] S.F. Betz, J.W. Bryson, W.F. DeGrado, Curr. Opin. Struct. Biol. 5 (1995) 457.
[34] R.S. Hodges, Biochem. Cell Biol. 74 (1996) 133.
[35] A. Lupas, Trends Biochem. Sci. 21 (1996) 375.
[36] R.A. Kammerer, Matrix Biol. 15 (1997) 555.
[37] W.D. Kohn, C.T. Mant, R.S. Hodges, J. Biol. Chem. 272 (1997) 2583.
[38] R.A. Kammerer, T. Schulthess, R. Landwehr, A. Lustig, J. Engel, U. Aebi, M.O. Steinmetz, Proc. Natl. Acad. Sci. USA 95 (1998) 13419.
[39] W.D. Kohn, R.S. Hodges, Trends Biotechnol. 16 (1998) 379.
[40] C. Micklater, J. Chmielewski, Curr. Opin. Chem. Biol. 3 (1999) 724.
[41] K. Wagschal, B. Tripet, R.S. Hodges, J. Mol. Biol. 285 (1999) 785.
[42] K. Wagschal, B. Tripet, P. Lavigne, C.T. Mant, R.S. Hodges, Protein Sci. 8 (1999) 2312.
[43] B. Tripet, K. Wagschal, P. Lavigne, C.T. Mant, R.S. Hodges, J. Mol. Biol. 300 (2000) 377.
[44] D.L. Lee, P. Lavigne, R.S. Hodges, J. Mol. Biol. 306 (2001) 539.
[45] P.C. Chong, R.S. Hodges, J. Biol. Chem. 257 (1982) 2549.
[46] R.S. Hodges, A.K. Saund, P.C. Chong, S.A. St.-Pierre, R.E. Reid, J. Biol. Chem. 256 (1981) 1214.
[47] S.Y.M. Lau, A.K. Taneja, R.S. Hodges, J. Biol. Chem. 259 (1984) 13253.
[48] R.S. Hodges, N.E. Zhou, C.M. Kay, P.D. Semchuk, Peptide Res. 3 (1990) 123.
[49] J.C. Hu, E.K. O'Shea, P.S. Kim, R.T. Sauer, Science 250 (1990) 1400.
[50] N.E. Zhou, C.M. Kay, R.S. Hodges, Biochemistry 31 (1992) 5739.
[51] N.E. Zhou, C.M. Kay, R.S. Hodges, J. Biol. Chem. 267 (1992) 2664.
[52] B.-Y. Zhu, N.E. Zhou, P.D. Semchuk, C.M. Kay, R.S. Hodges, Int. J. Pep. Protein Res. 40 (1992) 171.
[53] B.-Y. Zhu, N.E. Zhou, C.M. Kay, R.S. Hodges, Protein Sci. 2 (1993) 383.
[54] K.J. Lumb, P.S. Kim, Biochemistry 34 (1995) 8642.
[55] L. Gonzalez Jr., R.A. Brown, D. Richardson, T. Alber, Nat. Stuct. Biol. 3 (1996) 1002.
[56] L. Gonzalez Jr., J.J. Plecs, T. Alber, Nat. Stuct. Biol. 3 (1996) 510.
[57] L. Gonzalez Jr., D.N. Woolfson, T. Alber, Nat. Stuct. Biol. 3 (1996) 1011.
[58] O.D. Monera, F.D. Sönnichsen, L. Hicks, C.M. Kay, R.S. Hodges, Protein Eng. 9 (1996) 353.
[59] J. Moitra, L. Szilak, D. Krylov, C. Vinson, Biochemistry 36 (1997) 12567.
[60] E.K. O'Shea, R. Rutkowski, P.S. Kim, Science 243 (1984) 538.
[61] W.D. Kohn, C.M. Kay, R.S. Hodges, J. Mol. Biol. 267 (1997) 1039.
[62] W.D. Kohn, C.M. Kay, R.S. Hodges, J. Mol. Biol. 283 (1998) 993.
[63] Y.-H. Chen, J.T. Yang, K.H. Chau, Biochemistry 13 (1974) 3350.
[64] C.T. Chang, C.-S.C. Wu, J.T. Yang, Anal. Biochem. 91 (1978) 657.

[65] T.M. Cooper, R.W. Woody, Biopolymers 30 (1990) 657.
[66] J.W. Nelson, N.R. Kallenbach, Proteins 1 (1986) 211.
[67] J.W. Nelson, N.R. Kallenbach, Biochemistry 28 (1989) 5256.
[68] F.D. Sonnichsen, J.E. Van Eyk, R.S. Hodges, B.D. Sykes, Biochemistry 31 (1992) 8790.
[69] N.E. Zhou, C.M. Kay, R.S. Hodges, J. Biol. Chem. 267 (1992) 2664.
[70] N.E. Zhou, C.M. Kay, R.S. Hodges, Biochemistry 32 (1993) 3178.